1P4-5

Proceedings of Symposium on Ultrasonic Electronics, Vol. 30 (2009) pp. 95-96
18-20 November, 2009

Simulation of friction characteristics of ultrasonic motors lubricated with oil

油潤滑した超音波モータの摩擦特性シミュレーション

Kentaro Nakamura[1†] and Takaaki Ishii[2] ([1]P&I Lab., Tokyo Inst. of Tech; [2]Facult. Eng., Yamanashi Univ.)
中村健太郎 [1‡], 石井孝明 [2] （[1] 東工大 精研; [2] 山梨大 工）

1. Introduction

Ultrasonic motor has been developed by many groups for over two dicades, and gradually estalished sevral specific markets such as cameras, precise moving tables and instrumental equipments. However, the usage of ultrasonic motor has not been exploded yet. The major reason for this is the life.

In this report, we model the operation of ultrasonic motor in terms of the friction drive between the vibrator and the rotor. Then, oil is introduced into the friction interface, where we expect that the oil works as lubricant for the negative half cycle of the vibration and as traction enhancer for the positive half cycle. Being based on this idea, the motor performance is numerically simulated.

2. Simulation modeling

The essence of the operation mechanism of ultrasonic motor is represented by **Fig. 1**. Rotor is pressed to stator with the static preload. The stator generates two orthogonal vibration components: horizontal and vertical vibrations, the former drives the rotor to revolve through friction while the latter modulates the static preload at the ultrasonic frequency. If the vertical vibration *displacement* is synchronized with the horizontal vibration *velocity*, the friction force acts only for one direction and the horizontal vibration is rectified into the rotation of the rotor. This is the general mechanism of ultrasonic motor, and the two perpendicular components with the phase difference of 90 degrees are essential to the motor operation.

Next, let us introduce an electrical equivalent circuit model for simulating the operation. Friction characteristics and a rotor are connected for the load of an equivalent circuit model of a piezoelectric transducer[(1)] as shown in **Fig. 2**. The transducer is represented by the damped capacitance C_d and its loss R_d, the force factor A, and the mechanical resonance l_m, c_m, r_m. The force factor is a coefficient for the angular vibration velocity Ω to the motional current i_m as like in the step-up ratio of transformer: $i_m = A\Omega$, $T = AV$.

----

knakamur@sonic.pi.titech.ac.jp

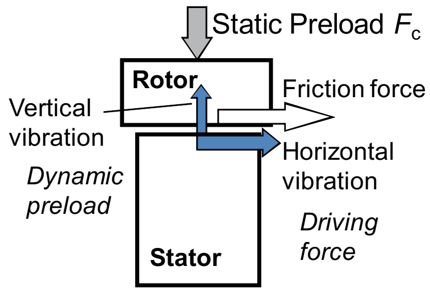

Fig. 1 Model of the operation of ultrasonic motor.

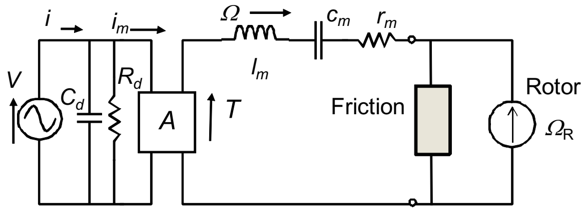

Fig. 2 Electrical equivalent circuit model for simulating the operation of Fig. 1.

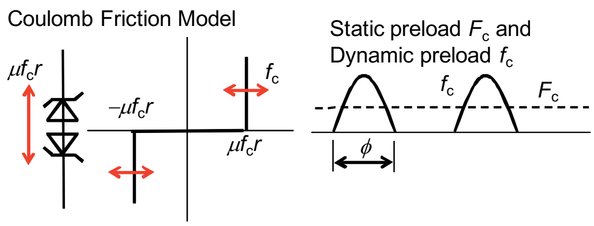

Fig. 3 Waveform of the dynamic preload and modeling of the conventional Coulomb friction.

Here, the rotor is denoted by a constant current source of rotor's angular velocity Ω_R, since the moment of inertia of therotor is large enough in comparison with the vibration frequency and the rotation speed is almost constant. More precisely, the rotor should be represented by an inductor equivalent to the rotor's inertia. The friction acting between the stator and the rotor is described by a twin Zener diode for representing the Coulomb friction as shown in **Fig. 3**. The element representing the friction is a shunt to the rotor to simulate the slip at the friction surface. The torque acting on the rotor is limited by the Zener voltage in the circuit. The twin-Zener diode is a bideirectional

Zener diode whose threchhold is changed by the dynamic preload f_c. The time-average of the dynamic preload shall be equel to the static preload F_c. The contact duration ϕ is defined in the figure.

3. Characteristics of oil

Instead of the conventional Coulomb friction, we introduce a model for ideal oil. We assume that a large traction force almost equal to the Coulomb friction is obtained under a large preload, while the friction is largely reduced when the preload is small. The former is like 'boundary lubrication' and the latter is 'hydrodynamic lubrication.' The characteristics is illustrated in **Fig. 4**. In the 'hydrodynamic' region, a film of oil is formed between the rotor and the stator, and it works as fluid to make a large slip and small force. In the 'boundary' region, the film is broken and a large traction is generated. The life would be better than the dry friciton because the damege due to slip becomes mild with the oil. If some kind of oil is used, the oil itself will transmit the traction force without breaking the oil film under very high preload since the oil will crystallized with the pressure in GPa oder.

4. Simulation results

Rotation speed was calculated as a function of the static preload for three different threshold between the hydrodynamic and boundary regions. The results are summarized in Fig. 5. As is expected, the rotor does not revolve at lower preload since the hydrodymanic condition is ocurred for whole period of the vibration. The rotor suddenly starts to revolve at a certain preload. The starting point is changed by the threshold of the friction condition. The similar phenomena was demonstrated in the experiment, where the surface roughness of the rotor was changed to simulate the different threshold of the friction condition. The results are shown in **Fig. 6**. A hybrid transducer type ultrasonic motor[2] with the diameter of 30 mm was used in the experiments. We obtained a good agreement between **Figs. 5** and **6** in qualitative meaning.

Next, the no-load revolution speed of the rotor was calculated as a function of the contact duration as shown in Fig. 7. The rotation speed is reduced as the contact duration if no oil is used. Lubrication has a significant effect on the rotor speed and efficiency if the contact duration is larger than 180 degrees.

5. Conclusion

Effect of the oil at the contact surface of ultrasonic motor was simulated in this report. The lubricant shall give an improvement in motor performance if the appropriate condition is chosen.

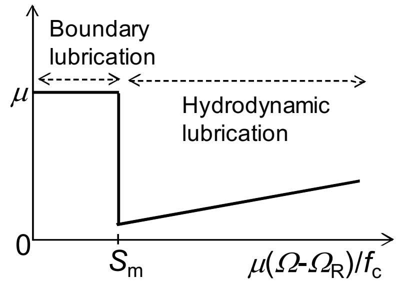

Fig. 4 Model of oil. Friction coefficient as functions of the slip and the dynamic preload.

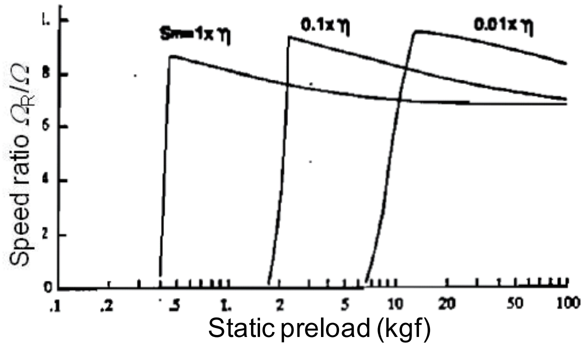

Fig. 5 Simulation results for the rotation speed.

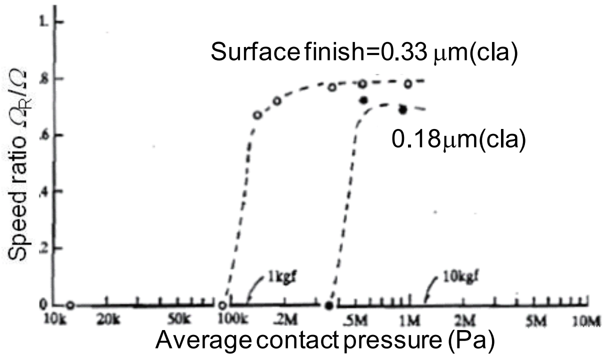

Fig. 6 Measured results for the rotation speed.

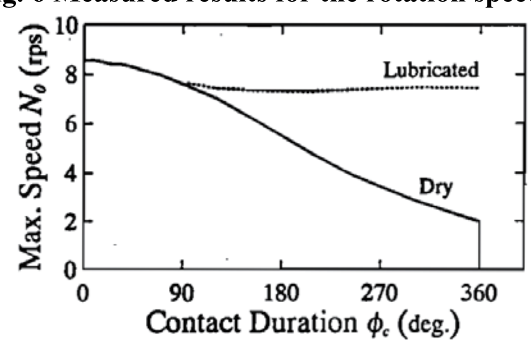

Fig. 7 Simulation results for the maximum rotation speed as a function of the contact duration.

References

1. K. Nakamura, M. Kurosawa and S. Ueha, *IEEE Trans. Ultrason. Ferroelec. Freq. Contr.*, **40** (1993) 402.
2. K. Nakamura, M. Kurosawa and S. Ueha, IEEE Trans. Ultrason. Ferroelec. Freq. Contr., **38** (1991) 188.